



Molecular modeling aided design of nicotinic acid receptor GPR109A agonists

Qiaolin Deng^{a,*}, Jessica L. Frie^b, Daria M. Marley^b, Richard T. Beresis^b, Ning Ren^c, Tian-Quan Cai^c, Andrew K. P. Taggart^c, Kang Cheng^c, Ester Carballo-Jane^d, Junying Wang^e, Xinchun Tong^e, M. Gerard Waters^c, James R. Tata^b, Steven L. Colletti^b

^a Department of Molecular Systems, Merck Research Laboratories, PO Box 2000, Rahway, NJ 07065, USA

^b Department of Medicinal Chemistry, Merck Research Laboratories, PO Box 2000, Rahway, NJ 07065, USA

^c Department of Cardiovascular Diseases, Merck Research Laboratories, PO Box 2000, Rahway, NJ 07065, USA

^d Department of Pharmacology, Merck Research Laboratories, PO Box 2000, Rahway, NJ 07065, USA

^e Department of Drug Metabolism, Merck Research Laboratories, PO Box 2000, Rahway, NJ 07065, USA

ARTICLE INFO

Article history:

Received 23 April 2008

Revised 8 August 2008

Accepted 11 August 2008

Available online 14 August 2008

Keywords:

GPR109A agonists

Homology modeling

ABSTRACT

A homology model of the nicotinic acid receptor GPR109A was constructed based on the X-ray crystal structure of bovine rhodopsin. An HTS hit was docked into the homology model. Characterization of the binding pocket by a grid-based surface calculation of the docking model suggested that a larger hydrophobic body plus a polar tail would improve interaction between the ligand and the receptor. The designed compounds were synthesized, and showed significantly improved binding affinity and activation of GPR109A.

© 2008 Elsevier Ltd. All rights reserved.

Nicotinic acid (Niacin) is a drug that has been extensively used in clinical practice for more than 50 years to reduce heart disease, by elevating high density lipoprotein cholesterol (HDL-C) and lowering low density lipoprotein cholesterol (LDL-C), triglycerides (TG) and free fatty acids (FFA).¹ However, it requires high dosages, and the beneficial effects are accompanied by the uncomfortable side effects of flushing (vasodilatation), which limits patient compliance. In 2003, three groups independently identified GPR109A, a G protein coupled receptor (GPCR), as a specific and high affinity receptor for nicotinic acid.² Two other receptors have been discovered that are related to GPR109A: GPR109B (89% sequence identity with GPR109A) which is a low affinity nicotinic acid receptor, and GPR81 (49% sequence identity with GPR109A). Given the well-demonstrated benefit of nicotinic acid, the discovery of nicotinic acid receptors has stirred great interest in pursuing GPR109A agonists,^{3,4} as potential therapeutic agents that might possess similar cardiovascular benefit to nicotinic acid while avoiding flushing.

GPR109A belongs to the family A GPCRs. GPCRs are trans-membrane proteins, sharing a common three-dimensional topology⁵ that consists of seven trans-membrane helices (7TMs) and one cytoplasmic helix, helix 8. The 7TMs are connected by three extra-cellular loops (ECLs) and three intra-cellular loops (ICLs). Sequence information for GPCRs is abundant, with ~9000 receptor sequences available. In contrast, structural information is limited

to two family A GPCRs: over 10 bovine rhodopsin structures determined from 2000 to date,^{6,7} and two human β_2 -adrenoceptor (β_2 AR) structures solved in 2007.⁸ The limited structural information makes molecular modeling of GPCRs as an important approach for structure–function studies and for drug design. The known X-ray crystal structures have provided attractive templates for homology modeling of family A GPCRs, and there are many examples in which the crystal structures of bovine rhodopsin have been successfully applied as templates.⁹

Here, we describe a molecular model of GPR109A bound to an anthranilic acid derivative, **1a** (Fig. 1), which was identified in a high throughput screen (HTS), and is a weak GPR109A agonist (Table 1). The homology model was constructed based on the X-ray crystal structure of bovine rhodopsin (PDB entry 1L9H), which was the best template at the time we carried out this study.⁷ Compound **1a** was docked into the putative binding pocket of GPR109A. Grid-based surface calculations of the docking model provided a clear visualization of the characterization of the binding pocket, which has aided design of compounds with significantly improved potency.

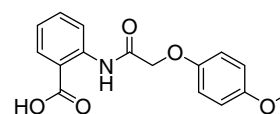


Figure 1. The chemical structure of the HTS hit, compound **1a**.

* Corresponding author. Tel.: +1 732 594 0618; fax: +1 732 594 4224.

E-mail address: qiaolin_deng@merck.com (Q. Deng).

Table 1

Compounds with a larger hydrophobic body have improved activity

Compound	R	[³ H]-nicotinic acid binding IC ₅₀ ^{a,b} (μM)	Human [³⁵ S]GTPγS EC ₅₀ ^b (μM)
Nicotinic acid	—	0.13	1.4
1a		33% at 25 μM 69% at 2.5 μM	12.5
1b		40% at 25 μM 78% at 2.5 μM	—
1c		1.2	1.2
1d		52% at 25 μM 88% at 2.5 μM	—
1e		0.14	1.0

^a Weak agonists were not subjected to full titrations and thus have no IC₅₀ determined. Instead, their bind % was reported at two concentrations here. Zero percent bound represents full competition.

^b Values are based on one or two experiments, each in triplicate and within 20% deviation. Missing data were due to inconclusive reading as a result of the curve shape.

In this report, each amino acid residue is represented by its amino acid name and original sequential number in the GPR109A sequence and then followed in parentheses by the TM number. For example, Arg111 on TM3 is described as Arg111(TM3) in the text.

A multiple sequence alignment of bovine rhodopsin with GPR109A, GPR109B, and GPR81 was generated by the program ClustalW¹⁰ with default parameters. After alignment by the program, manual adjustment was made to eliminate gaps in the helical region. The aligned 7TMs of GPR109A, GPR109B, and bovine rhodopsin are illustrated in Figure 2. GPR109A shares

about 20% identity and 58% similarity with bovine rhodopsin in the 7TM region. In all TMs, the most highly conserved residues (arrows in Fig. 2) are well aligned. Among GPCR A family members, a disulfide bond between TM3 and ECL2 (extra-cellular loop between TM4 and TM5) is well conserved. This disulfide bond remains in GPR109A, formed between Cys100(TM3) and Cys177(ECL2) (Fig. 3).

The homology model of GPR109A was constructed with the program Quanta/Modeler¹¹ based on the X-ray crystal structure of bovine rhodopsin (PDB entry 1L9H, 2.6 Å resolution).⁷ The N-terminal 22 residues and C-terminal 53 residues of GPR109A were excluded due to the lack of an available template for these

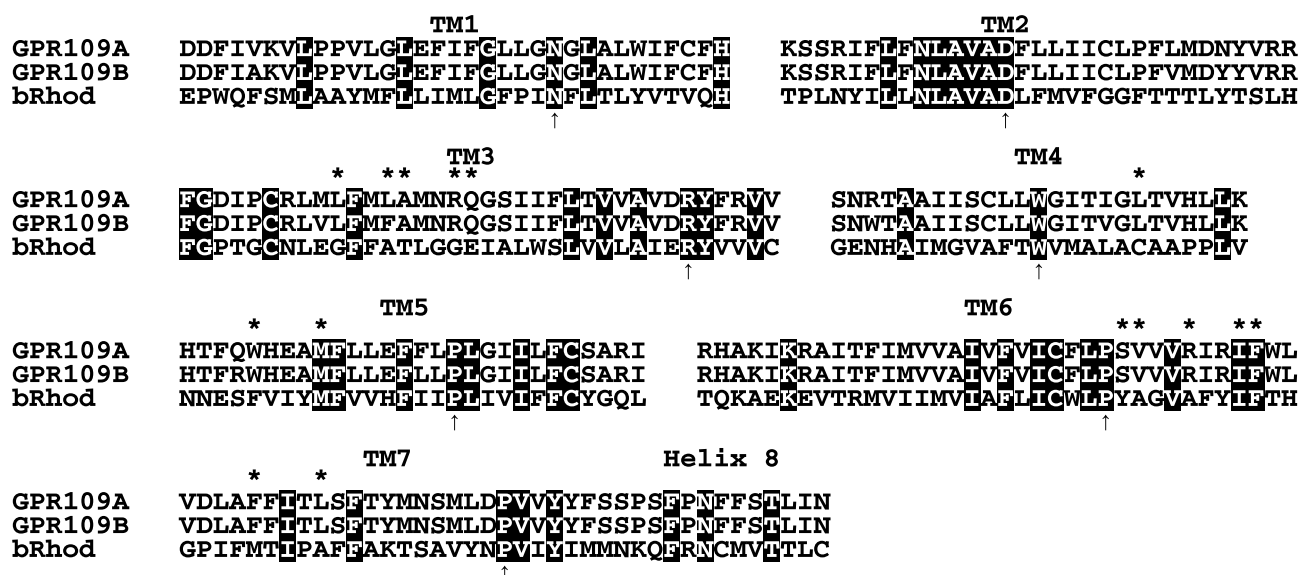


Figure 2. Sequence alignment of the 7TMs of GPR109A and GPR109B with bovine rhodopsin. Conserved residues are shown in black boxes. The most conserved residues in each TM are marked by an arrow. Asterisks above the alignment denote residues located within 4 Å of the ligand in the docking model of GPR109A bound to compound **1a**.

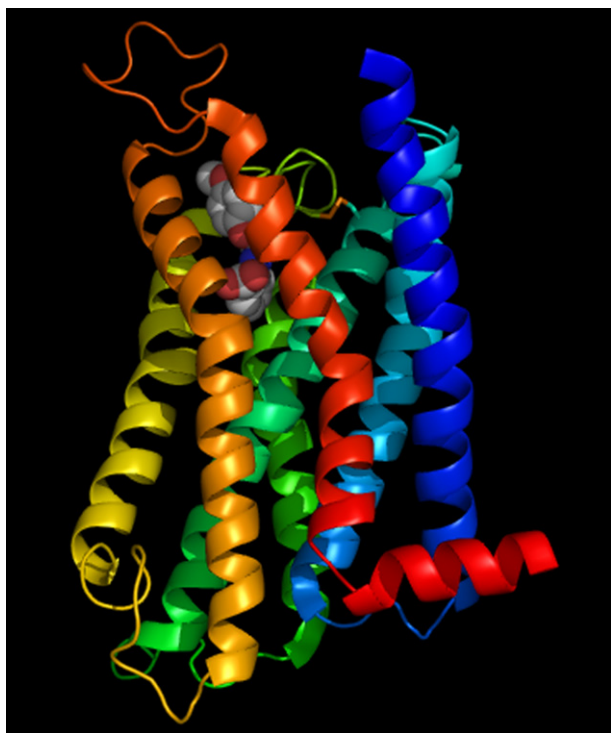


Figure 3. Docking model of GPR109A in complex with compound **1a**. The TM structures are shown as ribbon in rainbow color from TM1 (blue) to TM7 and helix 8 (red). The disulfide bond between TM3 and ECL2 is shown in an orange stick. The compound **1a** is shown in a spheres model, with carbon in gray, oxygen in red, and nitrogen in blue. The picture was prepared by PyMOL (Delano Scientific LLC, San Francisco, CA).

regions. The homology model generated by Modeler was further refined using molecular mechanics and molecular dynamics optimization to release strain. The quality of the model was validated by checking the geometry by Protein Health in Quanta.

Compound **1a** was docked into the homology model. One hundred conformations were generated using our implementation of the distance geometry approach.¹² The conformer set was energy minimized using a distance-dependent dielectric of $2r$ with the MMFFs force field.¹³ The compound prefers to adopt a linear conformation in the gas phase, with an intra-molecular hydrogen bond between the ortho carboxylate and NH group. Docking poses were generated by three methods: SQ,¹⁴ ICM,¹⁵ and LMOD.¹⁶ In SQ,¹⁴ the hundred conformations of compound **1a** were superimposed onto the retinal structure in 1L9H. The ICM docking program¹⁵ performs flexible docking in internal coordinates and generated a variety of docking poses. In LMOD,¹⁶ the program also performs flexible docking and produced a number of docking poses within a specified energy window. The poses obtained from all three methods were combined and the receptor–ligand complexes were subjected to energy optimization by the MMFFs force field. In the optimization, the ligand was fully minimized inside the binding pocket which allowed some degree of flexibility: the side chain of residues with any atom located within 5 Å of the ligand was fully optimized in conjunction with the ligand; residues falling within 5–10 Å of the ligand were included in the calculations as rigid elements; residues beyond 10 Å from the ligand were ignored in the calculations. The total energy of the complex, the individual energies of the ligand and the receptor, and the interaction energy between the ligand and the receptor were calculated. The best docking mode was determined by selecting poses with the most stabilizing interaction energy and minimal amount of strain of the ligand, and also by visual inspection of interactions between the ligand and the receptor.

Figure 3 illustrates the docking model of compound **1a** inside the GPR109A homology model. The ligand is bound in the TM helical bundle, close to the extra-cellular surface. The ligand is in an extended conformation and surrounded by residues mainly from TM3, TM5, TM6, and ECL2, and a few from TM4 and TM7. Amino acid residues in the 7TMs with any atom located within 4 Å of the ligand in the docking model are indicated with asterisks in Figure 2. In addition to these marked residues, there are a group of residues from ECL2 that also interact with the ligand directly.

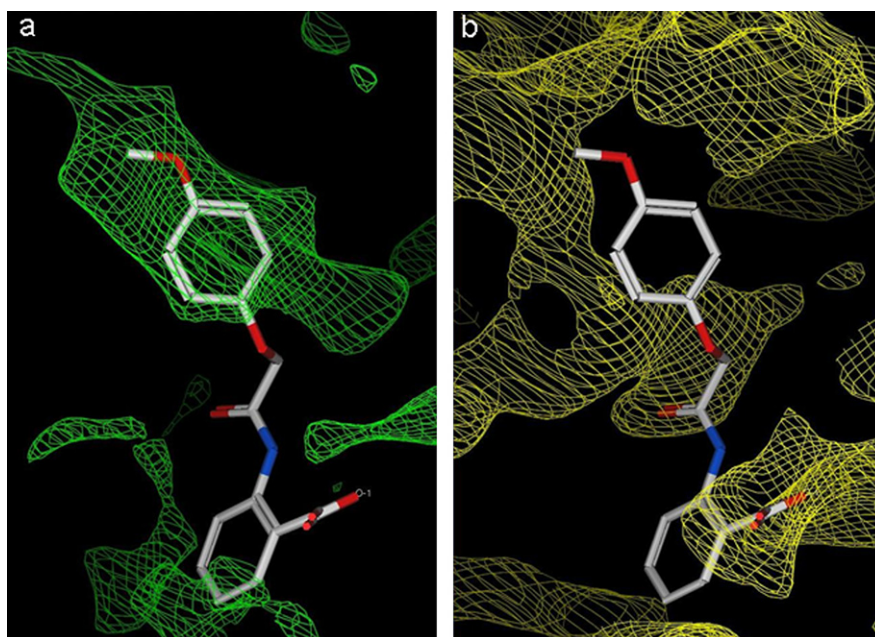
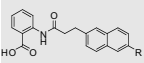


Figure 4. Contour maps from grid-based surface calculations of the docking model. (a) The hydrophobic contour is shown as a green grid. (b) The polar contour is shown as a yellow grid. The docked compound **1a** is shown in a stick model with carbon in gray, oxygen in red, and nitrogen in blue, while the nearby residues in the binding pocket are omitted.

Table 2

Compounds with a polar tail show enhanced activity

Compound	R	[³ H]-nicotinic acid binding IC ₅₀ ^a (μM)	Human [³⁵ S] GTPγS EC ₅₀ ^a (μM)
	—	0.13	1.4
1e	H	0.14	1.0
1f	OMe	0.087	1.25
1g	OH	0.024	0.38
1h	NH ₂	0.034	0.54
1i	CHO	0.055	0.94

^a Values are based on one or two experiments, each in triplicate and within 20% deviation.

Table 3Mouse pharmacokinetics of compound **1g**

Compound	Clp (mL/min/kg)	Vdss (L/kg)	T _{1/2} (h)	C _{max} (μM)	AUC _{norm} (μM h kg/mg)	F(%)
1g	6.2	0.7	3.2	6.6	8.3	55

Further examination of residues in the binding pocket identifies three groups of interactions. The first group consists of two arginines and one serine. Arg111(TM3) and Arg251(TM6) form salt bridges with the carboxylate in the ligand. Ser178(ECL2) is close to the amide carbonyl in the ligand and may form a hydrogen bond. These residues act as anchor points to direct the ligand to bind inside the binding pocket, and their importance has been validated by in-house mutagenesis data (not shown here) and in the literature.¹⁷ The second group of interactions involves hydrophobic residues that are located around the anisole moiety of the ligand, including Ile254(TM6), Phe255(TM6), and Phe276(TM7). The third group of interactions is formed by several polar residues at the mouth of the binding pocket, including Asn171(ECL2), Ser179(ECL2), and His259(ECL3), which are located in the flexible loop regions on the extra-cellular side and exposed to solvent.

Grid-based surfaces were calculated with our in-house program FLOG¹⁸ by using the docking model to further characterize the binding pocket. Each grid was visualized as a series of iso-energetic surfaces to portray the binding pocket by its hydrophobic and polar (hydrogen bond donor and acceptor) nature. Figure 4 depicts the hydrophobic and polar contour maps. For clarity, the ligand is shown, whereas the nearby residues are omitted in the picture. In the hydrophobic contour map (Fig. 4a), the extensive green area around the anisole denotes that this region in the binding pocket would favor interaction with a hydrophobic group on the ligand. Similarly, the large yellow area over the methoxy group indicates that this region, which is comprised of the polar residues located at the mouth of the binding pocket, would favor interaction with a polar group on the ligand.

Table 1 shows a series of compounds that test this docking model. The binding affinity of the compounds with the receptor was determined by competitive binding of compounds with the receptor against [³H]-nicotinic acid. Functional activities of the compounds were measured by a [³⁵S]GTPγS guanine nucleotide exchange assay.¹⁹

In Table 1, compound **1b** showed similar binding affinity as compound **1a**, indicating that the methoxy group has no favorable interaction with the binding pocket. Compound **1c** has a *tert*-butyl group to increase the hydrophobicity of the molecule, and thus enhanced its binding and activation. In the docking model, there is no direct interaction between the oxygen in the ether linker and the binding pocket, and this is demonstrated by the replacement with a carbon, that is, compounds **1d** and **1e**. Compound **1d** is still a weak agonist with a small hydrophobic body, while compound

1e is potent with a binding IC₅₀ of 0.14 μM and a [³⁵S]GTPγS EC₅₀ of approximately 1 μM. This compound can favorably match the hydrophobic map of the binding pocket of GPR109A. The compound is as potent as nicotinic acid and was used as a lead for further SAR development.

Based on compound **1e**, a series of compounds were synthesized with a polar substitution on the naphthyl ring in order to match the polar nature at the mouth of the binding pocket (Table 2). Compounds with hydrogen-bonding groups at the 6-naphthyl position showed improved potency. Both hydrogen bond donors and acceptors increased activity, presumably because the surrounding residues (Asn171, Ser179, and His259) can act as either hydrogen bond donors or acceptors. Among the compounds in Table 2, compound **1g**, with a hydroxyl group, is the most potent compound in the series, with a [³H]-nicotinic acid binding IC₅₀ of 24 nM and a [³⁵S]GTPγS EC₅₀ of 0.38 μM.

Compound **1g** is a full agonist of GPR109A and shows good bio-availability, half life, and oral exposure (Table 3). It significantly decreases plasma FFA in an in vivo pharmacodynamics assay in mice.^{3,4} Furthermore, treatment of mice with compound **1g** at 100 mpk resulted in a vasodilatation curve with an average AUC of 59 arbitrary units, whereas nicotinic acid, at the same dose, averaged 707 arbitrary units, indicating that compound **1g** did not induce vasodilatation.²⁰

In this report, we have documented a successful application of GPCR homology modeling for lead optimization. We constructed the GPR109A homology model based on the X-ray crystal structure of bovine rhodopsin in the unactivated dark state (PDB entry 1L9H). Recently, the X-ray crystal structures of activated forms of rhodopsin were released, including bathorhodopsin, lumirhodopsin, and a photoactivated deprotonated intermediate of rhodopsin.²¹ Given the high structural similarities between bovine rhodopsin in the dark state and the activated forms, the use of dark state rhodopsin as a modeling template is a reasonable starting point for homology modeling of family A GPCRs. Most recently, two X-ray crystal structures of human β₂-adrenoceptor (β₂AR) have been solved, providing non-rhodopsin templates for GPCR modeling.²² In the 7TM region, GPR109A shares 20% identity and 58% similarity with bovine rhodopsin, whereas it exhibits 19% identity and 55% similarity with β₂AR. Therefore, bovine rhodopsin appears a reasonable template for GPR109A modeling.

Based on the homology model of GPR109A, we docked the HTS hit **1a** into the binding pocket and further characterized the nature of the binding pocket using grid-based surface calculations. The hydrophobic and polar maps helped to understand the nature of the binding pocket and suggested that a larger hydrophobic body plus a polar tail in the ligand would improve its activity. Such compounds were synthesized, and showed significantly improved binding affinity and activation of GPR109A, resulting in a pharmacologically active compound **1g**.²³

References and notes

- Hotz, W. *Adv. Lipid Res.* **1983**, *20*, 195.
- (a) Tunaru, S.; Kero, J.; Schaub, A.; Wufka, C.; Blaukat, A.; Pfeffer, K.; Offermanns, S. *Nat. Med.* **2003**, *9*, 352; (b) Wise, A.; Foord, S. M.; Fraser, N. J.; Barnes, A. A.; Elshourbagy, N.; Eilert, M.; Ignar, D. M.; Murdock, P. R.; Steplewski, K.; Green, A.; Brown, A. J.; Dowell, S. J.; Szekeres, P. G.; Hassall, D. G.; Marshall, F. H.; Wilson, S.; Pike, N. B. *J. Biol. Chem.* **2003**, *278*, 9869; (c) Soga, T.; Kamohara, M.; Takasaki, J.; Matsumoto, S.; Saito, T.; Ohishi, T.; Hiyama, H.; Matsuo, A. *Biochem. Biophys. Res. Commun.* **2003**, *303*, 364.
- Shen, H. C.; Szymonifka, M. J.; Kharbanda, D.; Deng, Q.; Carballo-Jane, E.; Wu, K. K.; Wu, T.-J.; Cheng, K.; Ren, N.; Cai, T.-Q.; Taggart, A. K.; Wang, J.; Tong, X.; Waters, M. G.; Hammond, M. L.; Tata, J. R.; Colletti, S. L. *Bioorg. Med. Chem. Lett.* **2007**, *17*, 6723.
- Shen, H. C.; Ding, F.-X.; Luell, S.; Forrest, M. J.; Carballo-Jane, E.; Wu, K. K.; Wu, T.-J.; Cheng, K.; Wilsie, L. C.; Krsmanovic, M. L.; Taggart, A. K.; Ren, N.; Cai, T.-Q.; Deng, Q.; Chen, Q.; Wang, J.; Wolff, M. S.; Tong, X.; Holt, T. G.; Waters, M. G.; Hammond, M. L.; Tata, J. R.; Colletti, S. L. *J. Med. Chem.* **2007**, *50*, 6303.
- Fanelli, F.; De Denedett, P. G. *Chem. Rev.* **2005**, *105*, 3297.

6. Palczewski, K.; Kumasaka, T.; Hori, T.; Behnke, C. A.; Motoshima, H.; Fox, B. A.; Le Trong, I.; Teller, D. C.; Okada, T.; Stenlamp, R. E.; Yamamoto, M.; Miyano, M. *Science* **2000**, 289, 739.
7. Okada, T.; Fujiyoshi, Y.; Silow, M.; Navarro, J.; Landau, E. M.; Schichida, Y. *Proc. Nat. Acad. Sci. U.S.A.* **2002**, 99, 5982.
8. Cherezov, V.; Rosenbaum, D. M.; Hanson, M. A.; Rasmussen, S. G. F.; Thian, F. S.; Kobilka, T. S.; Choi, H.; Kuhn, P.; Weis, W. I.; Kobilka, B. K.; Stevens, R. C. *Science* **2007**, 318, 1258.
9. (a) Bosch, L.; Iarriccio, L.; Garriga, P. *Curr. Pharm. Des.* **2005**, 11, 2243; (b) Yates, A. S.; Doughty, S. W.; Kendall, D. A.; Kellam, B. *Bioorg. Med. Chem. Lett.* **2005**, 15, 3758; (c) Deng, Q.; Clemas, J. A.; Ghrebet, G.; Fischer, P.; Hale, J. J.; Li, Z.; Mills, S. G.; Bergstrom, J.; Mandala, S.; Mosley, R.; Parent, S. A. *Mol. Pharmacol.* **2007**, 71, 724.
10. Thompson, J. D.; Higgins, D. G.; Gibson, T. J. *Nucleic Acids Res.* **1994**, 22, 4673.
11. Sali, A.; Blindell, T. L. J. *Mol. Biol.* **1993**, 234, 779.
12. Crippen, C. M.; Havel, T. F. *Distance Geometry and Molecular Conformation*; Wiley: New York, 1988.
13. (a) Halgren, T. A. J. *Comp. Chem.* **1996**, 17, 490; (b) Halgren, T. A. J. *Comp. Chem.* **1996**, 17, 520; (c) Halgren, T. A. J. *Comp. Chem.* **1996**, 17, 553; (d) Halgren, T. A.; Nachbar, R. B. J. *Comp. Chem.* **1996**, 17, 587; (e) Halgren, T. A. J. *Comp. Chem.* **1996**, 17, 616; (f) Halgren, T. A. J. *Comp. Chem.* **1999**, 20, 720; (g) Halgren, T. A. J. *Comp. Chem.* **1999**, 20, 730.
14. Miller, M. D.; Sheridan, R. P.; Kearsley, S. K. J. *Med. Chem.* **1999**, 42, 1505.
15. Abagyan, R.; Totrov, M.; Kuznetsov, D. J. *Comp. Chem.* **1994**, 15, 488.
16. (a) Kolossvary, I.; Guida, W. C. J. *Comp. Chem.* **1999**, 20, 1671; (b) Keseru, G. M.; Kolossvary, I. J. *Am. Chem. Soc.* **2001**, 123, 12708.
17. Tunaru, S.; Lattig, J.; Kero, J.; Krause, G.; Offermanns, S. *Mol. Pharmacol.* **2005**, 68, 1271.
18. Miller, M. D.; Kearsley, S. K.; Underwood, D. J.; Sheridan, R. P. J. *Comput. Aided Mol. Des.* **1994**, 8, 153.
19. Taggart, A. K. P.; Kero, J.; Gan, X.; Cai, T.; Cheng, K.; Ippolito, M.; Ren, N.; Kaplan, R.; Wu, K.; Wu, T.-J.; Jin, L.; Liaw, C.; Chen, R.; Richman, J.; Connolly, D.; Offermanns, S.; Wright, S. D.; Waters, M. G. J. *Biol. Chem.* **2005**, 26649.
20. (a) Cheng, K.; Wu, T. J.; Wu, K. K.; Sturino, C.; Metters, K.; Gottesdiener, K.; Wright, S. D.; Wang, Z.; O'Neill, G.; Lai, E.; Waters, M. G. *Proc. Nat. Acad. Sci. U.S.A.* **2006**, 103, 6682; (b) Carballo-Jane, E.; Ciecko, T.; Luell, S.; Woods, J. W.; Zycband, E. I.; Waters, M. G.; Forrest, M. J. *Inflamm. Res.* **2007**, 56, 254.
21. (a) Nakamichi, H.; Okada, T. *Angew. Chem., Int. Ed.* **2006**, 45, 4270; (b) Nakamichi, H.; Okada, T. *Proc. Nat. Acad. Sci. U.S.A.* **2006**, 103, 12729; (c) Salom, D.; Lodowski, D. T.; Stenkamp, R. E.; Le Trong, I.; Golczak, M.; Jastrzebska, B.; Harris, T.; Ballesteros, J. A.; Palczewski, K. *Proc. Nat. Acad. Sci. U.S.A.* **2006**, 103, 16123.
22. Kobilka, B.; Schertler, G. F. X. *Trends Pharmacol. Sci.* **2008**, 29, 79.
23. Colletti, S. L.; Beresis, R. T.; Chen, W.; Tata, J. R.; Shen, H.; Marley, D. M.; Deng, Q.; Frie, J.; Ding, F.-X. PCT Patent Publication WO 2006/052555.